

# The location of the carboxy-terminal region of $\gamma$ chains in fibrinogen and fibrin D domains

(factor XIII/crosslinking/electron microscopy)

MICHAEL W. MOSESSON<sup>\*†</sup>, KEVIN R. SIEBENLIST<sup>\*</sup>, DAVID A. MEH<sup>\*</sup>, JOSEPH S. WALL<sup>‡</sup>, AND JAMES F. HAINFELD<sup>‡</sup>

<sup>\*</sup>Sinai Samaritan Medical Center, Milwaukee Clinical Campus, University of Wisconsin Medical School, Milwaukee, WI 53233; and <sup>‡</sup>Biology Department, Brookhaven National Laboratory, Upton, NY 11973

Communicated by John W. Suttie, University of Wisconsin, Madison, WI, June 29, 1998 (received for review March 20, 1998)

**ABSTRACT** Elongated fibrinogen molecules are comprised of two outer “D” domains, each connected through a “coiled-coil” region to the central “E” domain. Fibrin forms following thrombin cleavage in the E domain and then undergoes intermolecular end-to-middle D:E domain associations that result in double-stranded fibrils. Factor XIIIa mediates crosslinking of the C-terminal regions of  $\gamma$  chains in each D domain (the  $\gamma_{XL}$  site) by incorporating intermolecular  $\epsilon$ -( $\gamma$ -glutamyl)lysine bonds between amine donor  $\gamma 406$  lysine of one  $\gamma$  chain and a glutamine acceptor at  $\gamma 398$  or  $\gamma 399$  of another. Several lines of evidence show that crosslinked  $\gamma$  chains extend “transversely” between the strands of each fibril, but other data suggest instead that crosslinked  $\gamma$  chains can only traverse end-to-end-aligned D domains within each strand. To examine this issue and determine the location of the  $\gamma_{XL}$  site in fibrinogen and assembled fibrin fibrils, we incorporated an amine donor, thioacetyl cadaverine, into glutamine acceptor sites in fibrinogen in the presence of XIIIa, and then labeled the thiol with a relatively small (0.8 nm diameter) electron dense gold cluster compound, undecagold monoaminopropyl maleimide ( $Au_{11}$ ). Fibrinogen was examined by scanning transmission electron microscopy to locate  $Au_{11}$ -cadaverine-labeled  $\gamma 398/399$  D domain sites. Seventy-nine percent of D domain  $Au_{11}$  clusters were situated in middle to proximal positions relative to the end of the molecule, with the remaining  $Au_{11}$  clusters in a distal position. In fibrin fibrils, D domain  $Au_{11}$  clusters were located in middle to proximal positions. These findings show that most C-terminal  $\gamma$  chains in fibrinogen or fibrin are oriented toward the central domain and indicate that  $\gamma_{XL}$  sites in fibrils are situated predominantly between strands, suitably aligned for transverse crosslinking.

Fibrinogen molecules are  $\approx 45$  nm in length and are comprised of three major globular domains. There are two outer D domains, each connected by a “coiled-coil” region to the central E domain, within which the halves of each molecule are joined by disulfide bridges (Fig. 1). This article is concerned with precisely locating the carboxy-terminal segment of the  $\gamma$  chain, a region termed “ $\gamma_{XL}$ ”, that comprises one of several self-association sites in fibrinogen D domains (1). The  $\gamma_{XL}$  sequence contains one factor XIIIa amine donor/acceptor-crosslinking site between  $\gamma 406K$  and  $\gamma 398Q$  or  $\gamma 399Q$  [ $\gamma 398/399Q$ ] (2–4), as well as an overlapping platelet fibrinogen receptor-binding site lying between  $\gamma 400$  and  $\gamma 411$  (5).

To approach our objective, we prepared fibrinogen into which thioacetyl cadaverine amine donors had been covalently incorporated at glutamine acceptor sites in the presence of factor XIIIa (plasma transglutaminase) (Fig. 2). Subsequently,

we labeled the thiol group on the cadaverine with an electron dense thiol-specific gold-cluster compound, undecagold-monoaminopropyl maleimide ( $Au_{11}$ ) (6).  $Au_{11}$ -cadaverine-labeled fibrinogen was then examined by high resolution-scanning transmission electron microscopy (STEM) (7) to locate the  $Au_{11}$  clusters that had been covalently attached at the amine acceptor site ( $\gamma 398/399Q$ ) in the D domain. The relatively small diameter (0.8 nm) of the  $Au_{11}$  cluster (6) provides a discriminating ultrastructural probe for pinpointing its position in the fibrinogen molecule. Gold cluster labeling has been applied to several proteins or nucleic acids for topographical molecular mapping of specific binding sites or domains (7–11 *inter alia*) and in particular has been used to determine precisely the location as well as the orientation of the amino terminal portions of the two  $A\alpha$  chains within each fibrinogen E domain (12).

The C-terminal region of each  $\gamma$  chain contains a single crosslinking site at which factor XIIIa catalyzes the formation of  $\gamma$  dimers (1, 13, 14) by incorporating intermolecular reciprocal  $\epsilon$ -( $\gamma$ -glutamyl) lysine bridges between a donor  $\gamma 406$  lysine of one chain and a glutamine acceptor at  $\gamma 398/399$  of another (2–4).  $\gamma$  chain crosslinking occurs solely between these residues (2–4, 15, 16), whereas there are several amine donor lysine and amine acceptor glutamine sites in  $A\alpha$  chains (16, 17). Primary amine compounds like cadaverine are competitive amine donor substrates that become specifically incorporated in the presence of factor XIIIa at the single  $\gamma$  chain acceptor site or at one or more  $\alpha$  chain acceptor sites (2–4, 15, 18, 19).

Noncovalent interaction between D and E domains in an assembling fibrin polymer facilitates the antiparallel intermolecular alignment of  $\gamma$  chain pairs in D domains, thereby accelerating the rate at which factor XIIIa-catalyzed crosslinking occurs at  $\gamma_{XL}$  sites (1, 14). Since the report by Fowler *et al.* (20), which involved electron microscopic observations on crosslinked fibrinogen dimers, it has been commonly held that the C-terminal  $\gamma$  chain crosslinking sequences in fibrin are situated at the extreme end of each molecule, bridging directly between end-to-end abutted fibrin molecules in a so-called “DD-long” arrangement. Recently, the “end-to-end” crosslinking idea received somewhat revised support from studies of crystals of crosslinked D dimer fragments (21), in which crosslinked C-terminal  $\gamma$  chains, though not situated at the extreme end of the molecule as originally envisioned, were inferred nevertheless to traverse the abutting D domains in an end-to-end alignment. However, several independent lines of evidence, beginning with reports by Selmayr *et al.* (22, 23), have indicated that the crosslinked  $\gamma$  chain segments in fibrin do not straddle the ends of adjacent D domains but rather tend

The publication costs of this article were defrayed in part by page charge payment. This article must therefore be hereby marked “advertisement” in accordance with 18 U.S.C. §1734 solely to indicate this fact.

© 1998 by The National Academy of Sciences 0027-8424/98/9510511-6\$2.00/0  
PNAS is available online at [www.pnas.org](http://www.pnas.org).

Abbreviations: STEM, scanning transmission electron microscopy;  $Au_{11}$ , undecagold-monoaminopropyl maleimide; ATA, *N*-[(acetylthio) acetyl]; HBS, Hepes-buffered saline; TA, thioacetyl.

<sup>†</sup>To whom reprint requests should be addressed. e-mail: [mosesson@facstaff.wisc.edu](mailto:mosesson@facstaff.wisc.edu).

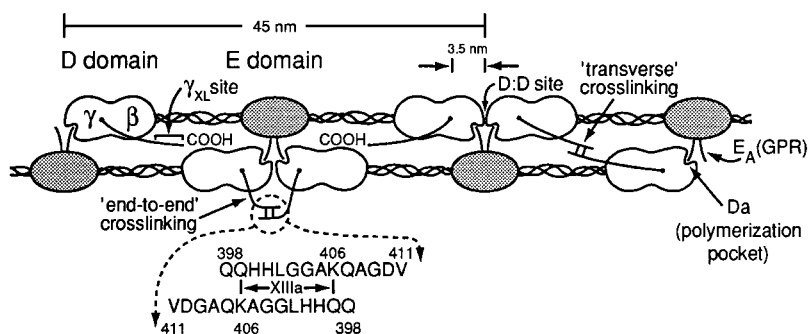


Fig. 1. Schematic diagram of the 45 nm long fibrin(ogen) molecule includes information that helps to frame the issue of the location of the C-terminal region of the  $\gamma$  chain. End-to-middle assembly of fibrin molecules to form half-staggered double-stranded fibrils is shown, illustrating the polymerization site interaction (Da:E<sub>A</sub>) that governs the assembly process. The crosslinking arrangement of  $\gamma_{XL}$  sites of  $\gamma$  chains in transverse or end-to-end orientations is shown, as is the C-terminal sequence of the  $\gamma$  chain from  $\gamma_{398}$  to the C-terminus at  $\gamma_{411}$ . The terminal portion of the  $\gamma$  chain emerges 3.5 nm from the distal end of each molecule (27). The positioning of end-to-end-crosslinked  $\gamma$  chains has been adjusted from the originally proposed location at the extreme ends of the D domain (DD-long; ref. 20) to take into account recent data indicating that their location at the D:D site is not a realistic possibility (1, 21, 25, 27).

to extend transversely between each fibril strand (1, 24–26). Evidence in favor of the transverse bond arrangement includes among the above cited articles, the electron microscopic demonstration of double-stranded crosslinked fibrinogen fibrils, visualization of bridging filaments representing transversely positioned  $\gamma$  chains within crosslinked fibrinogen fibrils (1) and in crosslinked D-fibrin-D complexes (26), and evidence indicating that the abutting ends of fibrin D domains where end-to-end intermolecular contacts are now recognized to occur (the so-called D:D site) (1, 21, 25), do not as first proposed (20), contain the C-terminal  $\gamma$  chain segment. Crystallographic analyses of D domain structures (21, 27) have amply confirmed the last conclusion by showing that the C-terminal region of the  $\gamma$  chain emerges from the middle of the  $\gamma$  chain segment of the D domain 3.5 nm from its extreme end (Fig. 1).

The compelling evidence for transverse crosslinking notwithstanding, both crystallographic reports (21, 27) have argued instead, based on data derived from their D domain fragment structures, that in native fibrin polymers only end-to-end crosslinking is possible. This inference stems from a calculation that the C-terminal region of the  $\gamma$  chain cannot possibly bridge the distance required to link two transversely

aligned  $\gamma$  chains in an assembled fibrin polymer. More recent reports on single-stranded crosslinked fibrinogen fibrils formed on a fibrin fragment E template (28) or a duplex gly-pro-arg-pro fragment E-like template (29), also have offered evidence for end-to-end crosslinking, and Veklich *et al.* (28) have inferred from these observations that the same is universally true of the crosslinking that occurs in native assembled fibrin polymers. This general issue will be considered in more detail later, but it will suffice to state at this point that we undertook the gold cluster mapping project described here to further assess the possibility of transverse versus end-to-end crosslinking in ordered polymers of fibrinogen and fibrin.

## MATERIALS AND METHODS

**Fibrinogen.** Fraction I-9 fibrinogen was prepared as described (30). Fibrinogen molecules in this preparation lack  $\approx 100$  or more C-terminal A $\alpha$  chain residues (31), which contain almost all of the lysine amine donor sites (16, 17), and therefore they do not participate in  $\alpha$  chain crosslinking of fibrin (32).  $\gamma$  chain dimerization is, however, slightly slower but otherwise normal (1). Human  $\alpha$ -thrombin (specific activity, 3.04 units/ $\mu$ g) was obtained from Enzyme Research Laboratories (South Bend, IN).

**Factor XIII and Its Activation to Factor XIIIa.** Plasma factor XIII was prepared as described by Lorand and Gotoh (33) and had a specific activity of 2,460 Loewy units/mg (34). Factor XIII was activated to XIIIa at a concentration of 1,000 units/ml in 100 mM NaCl, 50 mM Hepes, pH 7 buffer containing 500  $\mu$ M DTT by the addition of thrombin (final concentration, 5 units/ml). After activation for 30 min at 37°C, a 10-fold excess of hirudin (50 units/ml; Sigma) was added to inhibit the thrombin. The activated XIIIa preparation was then diluted for use in cadaverine incorporation or fibrinogen-crosslinking experiments.

**Synthesis of N-[(acetylthio)acetyl]-Cadaverine (ATA-Cadaverine).** ATA-cadaverine, the starting material for fibrinogen-labeling cadaverine derivatives, was prepared by mixing N-succinimidyl-S-acetylthioacetate (SATA, Calbiochem) in dimethyl sulfoxide in equimolar amounts (430 mM each) with cadaverine (1,5-diaminopentane) (Sigma) containing 1,5-<sup>14</sup>C cadaverine (14.9 mCi/mmol) (Sigma) in 50 mM Hepes, pH 7.0 buffer, to yield a solution having a final concentration of 120 mM with respect to each reacting component. After overnight incubation at room temperature, 3 ml of the mixture (3.6  $\mu$ mol of each) was diluted with an equal volume of water and loaded onto a 1.5  $\times$  30 cm column of carboxymethyl-Sephadex (Pharmacia Biotech, Piscataway, NJ) that had been equili-

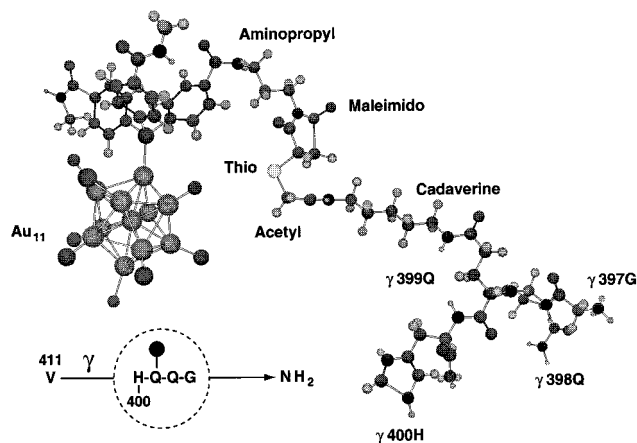


Fig. 2. A molecular ball-and-stick scale model of the Au<sub>11</sub> cadaverine compound linked to the  $\gamma$  chain at Gln-399 through an  $\epsilon$ -( $\gamma$ -glutamyl)lysine bond. The organic structure has a contour length of 2.7 nm, and its constituent groups are listed. In the conformation shown, the 0.8 nm diameter Au<sub>11</sub> cluster is  $\approx 1.5$  nm from the  $\gamma$  Gln side chain and is an extended version that was obtained by using an energy minimization procedure (Chem 3D). A schematic drawing showing the general orientation of the cluster compound along the  $\gamma$  chain is given in the lower portion of the diagram.

brated with 20 mM Hepes and 5 mM NaCl, pH 7.0 buffer. The column was developed with a linear gradient by using a limit buffer of 600 mM NaCl and 20 mM Hepes, pH 7.0. Three peaks containing  $^{14}\text{C}$  radioactivity emerged, and the chromatographic fractions (3.0 ml each) were assayed for the presence of thiol groups with 5,5'-dithiobis-(2-nitrobenzoic acid) (DTNB; Sigma) both before and after treatment with 100 mM hydroxylamine ( $\text{NH}_2\text{OH}$ ) to deprotect the acetylated thiol group. The first eluted peak contained doubly labeled *N,N*-di ATA-cadaverine, the second, monovalent *N*-ATA-cadaverine, and the third, unreacted cadaverine.

**Incorporation of Thioacetyl Cadaverine into Fibrinogen, Labeling Fibrinogen with  $\text{Au}_{11}$ , and Preparation of Fibrin Fibrils.** Thioacetyl cadaverine (TA-cadaverine) was prepared by treating ATA-cadaverine with 100 mM hydroxylamine to remove the protecting acetyl group. After deprotection, the mixture was passed over a 10-ml mercury-containing column of Affi-Gel 501 resin (Bio-Rad) to bind the TA-cadaverine and separate it from non-thiol-containing molecules and then eluted with 25 ml (2.5-column volumes) of 50 mM  $\text{NH}_4\text{HCO}_3$  and 10 mM  $\beta$ -mercaptoethanol, pH 7.4. The pooled TA-cadaverine sample was then taken to dryness in a freeze dryer.

TA-cadaverine was incorporated into fibrinogen in 50 mM Hepes, 50 mM NaCl, and 10 mM  $\text{CaCl}_2$ , pH 7.4 buffer at a molar ratio of cadaverine to fibrinogen of 1,000:1 and a factor XIIIa level of 50 units/ml. After 30 min at 25°C, the crosslinking reaction was terminated by addition of EDTA (25 mM, final). Under these conditions, 1.65 mol of TA-cadaverine was incorporated per mol of fibrinogen. After incorporation into fibrinogen, the mixture was reacted overnight with a fivefold molar excess of  $\text{Au}_{11}$ -monoaminopropyl maleimide that had been prepared as described (6), and the mixture then passed over a Superose 12 (Pharmacia Biotech, Piscataway, NJ) gel-sieving column to separate fibrinogen from the unbound  $\text{Au}_{11}$  cluster.  $\text{Au}_{11}$ -cadaverine-labeled fibrinogen emerged in two peaks, the first of which was small (<10%) and contained crosslinked dimeric and oligomeric fibrinogen molecules and the second, mostly fibrinogen monomers. Control electron microscope experiments to detect bound  $\text{Au}_{11}$  clusters were carried out on fibrinogen isolated from mixtures of fibrinogen and  $\text{Au}_{11}$ -monopropylamine (i.e., without maleimide "activation") by gel sieving as described above.

The monomeric  $\text{Au}_{11}$ -fibrinogen fraction obtained by gel sieving was diluted to a concentration of 20  $\mu\text{g}/\text{ml}$  in 300 mM NaCl and 50 mM Hepes (pH 7.4) buffer with thrombin added (2 units/ml, final); the mixture was incubated at room temperature for 30 min, then mixed back and forth in a pipette tip, and applied to the surface of a grid.

**Preparation of Crosslinked Fibrinogen Fibrils from  $\text{Au}_{11}$ -Cadaverine-Labeled Fibrinogen.** The monomeric  $\text{Au}_{11}$ -fibrinogen fraction obtained by gel sieving was subjected to crosslinking in the presence of factor XIIIa (50 units/ml) for 20 min at a fibrinogen concentration of 100  $\mu\text{g}/\text{ml}$  in 150 mM NaCl, 10 mM  $\text{CaCl}_2$ , and 10 mM Hepes, pH 7.4 buffer containing 100  $\mu\text{M}$  DTT. After this incubation period, the mixture was mixed back and forth in a pipette tip, diluted to a fibrinogen concentration of 5  $\mu\text{g}/\text{ml}$  in 10 mM Hepes and 150 mM NaCl, pH 7.4 buffer (HBS), and applied to the grid for microscopy in the usual way.

In some experiments,  $\text{Au}_{11}$ -fibrinogen was mixed with an equal amount of unlabeled fibrinogen to yield a final fibrinogen concentration of 240  $\mu\text{g}/\text{ml}$  in HBS containing 10 mM  $\text{CaCl}_2$ . Factor XIIIa was added to this mixture (100 units/ml, final), incubated for 20 min at room temperature, mixed back and forth in pipette tip, and diluted with HBS for application to a microscope grid.

**Preparation of  $\text{Au}_{11}$ -Thioacetyl Cadaverine Before Incorporation into Fibrinogen.** In one set of experiments,  $\text{Au}_{11}$ -TA-cadaverine was prepared from TA-cadaverine by reacting it overnight with  $\text{Au}_{11}$ -monoaminopropyl maleimide at a 1:1 M

ratio in a 150 mM NaCl, 13 mM phosphate, and 1 mM EDTA, pH 7 buffer. The reaction mixture was centrifuged over a Centricon 3 filter (Amicon) in a 100 mM NaCl and 50 mM Hepes, pH 7 buffer to separate unreacted components from the gold compound. The  $\text{Au}_{11}$ -TA-cadaverine was incubated at a 10:1 M ratio for 30 min with fibrinogen at 1 mg/ml in the presence of factor XIIIa (35 units/ml). After the incubation period, *N*-ethyl maleimide was added (10 mM, final) to inhibit factor XIIIa, and the mixture was centrifuged over a Centricon 30 membrane filter to separate unbound  $\text{Au}_{11}$ -TA-cadaverine from the fibrinogen.

**Preparation of Samples for STEM.** Samples for STEM were diluted, usually in HBS, to the desired protein concentration (typically 2–20  $\mu\text{g}/\text{ml}$ ), loaded onto ultrathin carbon films by injecting the specimen into a droplet on the grid surface in the sample buffer and allowing an attachment time of 1 min before exchanging the fluid on the grid surface by multiple wicking, and washing with 150 mM ammonium acetate, pH 7. The grid was then rapidly frozen in degassed liquid nitrogen, freeze-dried, and transferred to the STEM microscope stage under vacuum. Specimens were imaged at the Brookhaven STEM Biotechnology Resource Facility by using a 40-kV probe focused at 0.25 nm. The images were stored digitally as a raster of  $512 \times 512$  pixels. For imaging gold clusters within fibrinogen or fibrin, we used magnifications of  $500,000 \times$  (128 nm full scan width) at an electron dose of  $\approx 1 \times 10^4 \text{ e}^-/\text{nm}^2$ , whereas for identifying areas containing a good distribution of fibrinogen molecules or fibers, a lower magnification of  $125,000 \times$  (512 nm full scan width) at an electron dose of  $\approx 2.5 \times 10^3 \text{ e}^-/\text{nm}^2$ .

## RESULTS

### General Considerations for Studying $\text{Au}_{11}$ -Fibrinogen.

Our initial strategy for preparing  $\text{Au}_{11}$ -cadaverine-labeled fibrinogen was to incorporate ATA-cadaverine directly into fibrinogen in the presence of factor XIIIa, remove the protecting acetyl group by treatment with hydroxylamine, and then label the exposed thiol group with the gold maleimide compound. However, hydroxylamine treatment caused irreversible fibrinogen precipitation, and we soon abandoned that approach in favor of directly incorporating TA-cadaverine into fibrinogen and then labeling the sulfhydryl groups in fibrinogen with  $\text{Au}_{11}$ -maleimide. For some experiments, we prepared  $\text{Au}_{11}$ -cadaverine for direct incorporation into fibrinogen, but the amount we obtained was small, making it difficult to attain the high molar ratio of cadaverine to fibrinogen that is

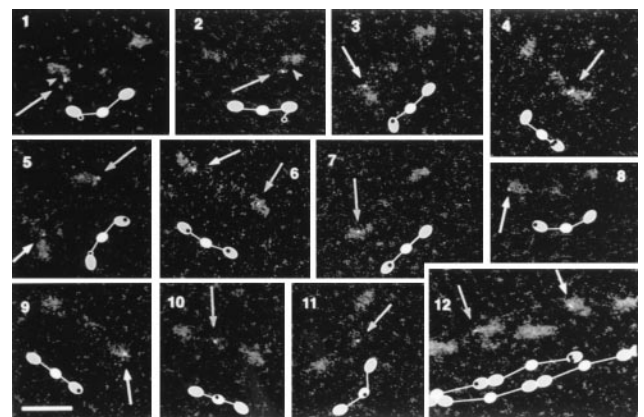


FIG. 3. A gallery of  $\text{Au}_{11}$  cluster-labeled fibrinogen molecules. Occasional monoamino  $\text{Au}_{11}$  cluster structures contain two  $\text{Au}_{11}$  clusters (e.g., molecules 4 and 12). Arrows indicate  $\text{Au}_{11}$  cluster locations. Arrowheads (molecules 1 and 2) indicate a filamentous connection between the  $\text{Au}_{11}$  cluster and the D domain. A caricature of each molecule is provided for clarity. (Bar = 20 nm.)



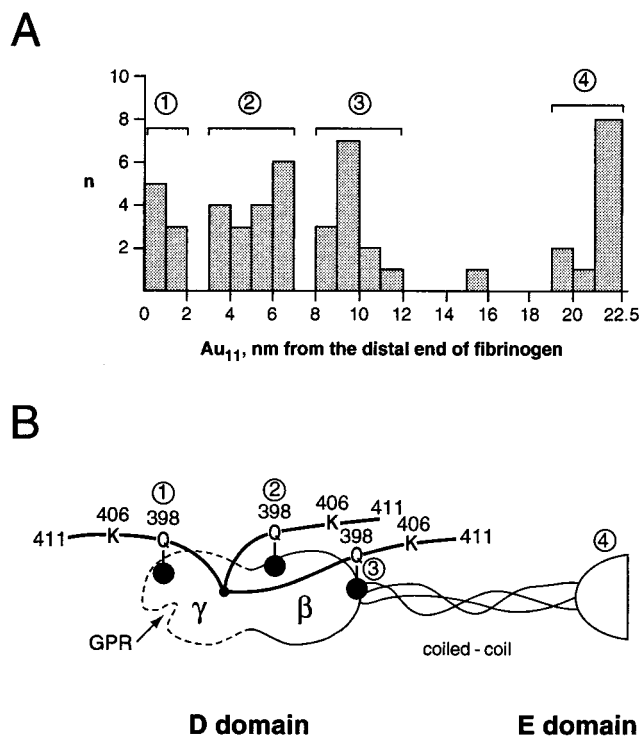


FIG. 4. A histogram showing the distribution of Au<sub>11</sub> clusters on fibrinogen molecules (A) and an aligned diagram of a fibrinogen half-molecule illustrating the orientation of the C-terminal  $\gamma$  chain in the fibrinogen D domain (B). Gold clusters were distributed in four locations on the molecule: 1, distal D domain; 2, middle D domain; 3, proximal D domain; and 4, E domain. The gold clusters (●) that label the  $\gamma$  chains at  $\gamma$ 398Q or  $\gamma$ 399Q are designated simply as “398.”

necessary to obtain efficient cadaverine incorporation. Nevertheless, we were able to compare Au<sub>11</sub>-cadaverine-labeled fibrinogen with structurally equivalent Au<sub>11</sub>-maleimide-labeled TA-cadaverine fibrinogen (hereafter designated simply “Au<sub>11</sub>-fibrinogen”) by STEM, and although many fewer examples of Au<sub>11</sub>-cadaverine-labeled fibrinogen molecules were found, the distribution of Au<sub>11</sub> label in these structures was essentially the same as for the second type of Au<sub>11</sub>-fibrinogen (data not shown).

To detect the relatively small Au<sub>11</sub> clusters (diameter 0.8 nm) within fibrinogen molecules, we imaged specimens at high magnification (500,000 $\times$ ; 0.25 nm/pixel) after first locating promising areas on the grid surface at lower magnifications (e.g., 125,000 $\times$ ; 1 nm/pixel). At the higher magnification, Au<sub>11</sub> clusters can be detected at a sufficiently low electron dose ( $\approx 1 \times 10^4$  e<sup>-</sup>/nm<sup>2</sup>) that significant biological structure is preserved, although the E domains and the coiled-coil regions of fibrinogen molecules were often not well visualized above the background carbon film. Nevertheless, there was no difficulty in identifying fibrinogen molecules and in determining the position of the Au<sub>11</sub> clusters within them.

**Au<sub>11</sub>-Cadaverine-Labeled Fibrinogen.** Au<sub>11</sub>-fibrinogen showed a relatively high percentage of gold-labeled molecules ( $\approx 25\%$  of the total observed). Control experiments with “unactivated” Au<sub>11</sub>-monopropylamine revealed no evidence of nonspecific fibrinogen labeling by the Au<sub>11</sub> cluster (data not shown). Many examples of singly labeled gold cluster-labeled fibrinogen molecules were found, and occasionally we found gold clusters at both ends of a molecule (Fig. 3, molecules 5 and 6). Most gold clusters were situated in the D domain (76%), indicating  $\gamma$  chain labeling at Gln-398/399. Au<sub>11</sub> clusters found in the vicinity of the E domain (Fig. 3, molecules 10 and 11) corresponded to Au<sub>11</sub>-cadaverine labeling of A $\alpha$  chain Gln acceptor sites. Of the Au<sub>11</sub>-labeled molecules in the D domain, 79% were located 3–12 nm from the distal end of the D domain, and the remaining 21% were positioned in the distal end of the D domain (Fig. 4). Au<sub>11</sub> cluster distribution within the D domain fell into three categories relative to the extreme end of the molecule—distal (0–2 nm; Fig. 3, molecules 5, 8, and 9); middle (3–7 nm; Fig. 3, molecules 4, 6, 7, and 12); and proximal regions (8–12 nm; Fig. 3, molecules 1, 2, 3, 5, and 6).

We considered the position of the Au<sub>11</sub> cluster in relation to the labeled  $\gamma$ 398/399 site at which cadaverine is incorporated in the presence of factor XIIIa. Molecular modeling of the organic structure (Fig. 2), which has a contour length of 2.7 nm, by an energy minimization procedure (Chem 3D, Cambridge-Soft), indicates that it is curvilinear, and the Au<sub>11</sub> is situated 0.9 to 1.5 nm from the terminal amine of the  $\gamma$ -glutamyl side chain. Thus, the actual position of  $\gamma$ 398/399 is most likely within 1.5 nm or less of the measured position of the Au<sub>11</sub> cluster itself.

Au<sub>11</sub> clusters in the middle region of the D domain were close to the point of emergence of the C-terminal region of the  $\gamma$  chain, 3.5 nm from the distal end of the molecule (27), suggesting that these  $\gamma$  chain C-terminal regions are aligned more-or-less perpendicular to the longitudinal axis of the molecule, or possibly also fold or bend after they emerge from the D domain. Nevertheless, for the most part, those regions of the  $\gamma$  chain 4 nm or more from the distal end, also are oriented away from rather than toward the distal region of the molecule. Clusters situated at the distal end of the D domain (21% of the total) no doubt reflect  $\gamma$  chains that are oriented toward the far end of the molecule and/or that also bend somewhat from their point of origin in the middle of the  $\gamma$  subdomain (Fig. 4).

**Incorporating Au<sub>11</sub>-Fibrinogen into Crosslinked Fibrinogen Fibrils.** We attempted to prepare crosslinked fibrinogen fibrils by adding factor XIIIa to Au<sub>11</sub>-fibrinogen or to unlabeled fibrinogen. In unlabeled fibrinogen crosslinking mixtures, we observed many typical examples of elongated double-stranded fibrinogen fibrils (not shown). In contrast, in Au<sub>11</sub>-fibrinogen crosslinking mixtures, most polymeric structures did not form the expected double-stranded fibrils, and thus their molecular organization was difficult to interpret. Occasionally, we found some short though interpretable protofibrillar structures (i.e., five to ten fibrinogen molecules), and when Au<sub>11</sub>-fibrinogen molecules were incorporated into these

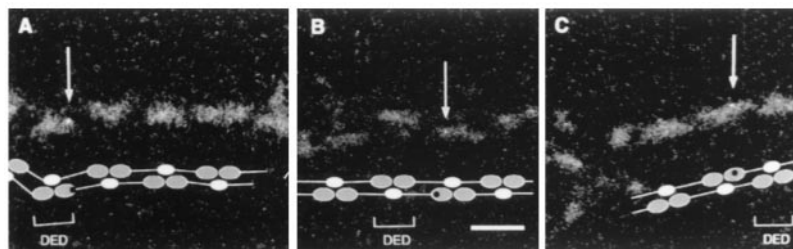


FIG. 5. Au<sub>11</sub> cluster labeling in fibrin fibrils. Several examples of double-stranded fibrin fibrils labeled with Au<sub>11</sub> clusters are shown. A diagram showing the molecular arrangement in each fibril is provided for clarity. (Bar = 20 nm.)

structures (Fig. 3, molecule 12), Au<sub>11</sub> clusters were found in middle to proximal regions of the D domains, just as in monomeric fibrinogen molecules themselves.

The failure to incorporate Au<sub>11</sub>-fibrinogen into well organized two-stranded fibrils relates to the fact that reactive  $\gamma$  chain-crosslinking sites in fibrinogen are required for proper fibrinogen fibril formation (1). Because most of these sites had been used by the cadaverine labeling process itself, Au<sub>11</sub>-cadaverine-labeled fibrinogen molecules have a limited capacity to participate in fibril formation. In a sense, this negative result supports the basis for formation of crosslinked fibrinogen fibrils through transverse  $\gamma_{XL}$  site interactions.

**Incorporating Au<sub>11</sub>-Labeled Fibrinogen into Fibrin.** We prepared fibrin clots under high ionic strength conditions favoring thin fibril formation, and we were able to find several fibrils into which one or more Au<sub>11</sub>-labeled fibrin molecules had been incorporated (Fig. 5). Gold clusters in these fibrils were located in middle to proximal regions of the D domains comprising the fibril DED complex. An occasional gold cluster was found in the E domain (1 of 8 incorporated clusters observed), but none was observed at the distal end of a D domain.

## DISCUSSION

Solution NMR studies and analyses of "stabilized" crystals from the C-terminal regions of the  $\gamma$  chain indicate that this region can assume multiple conformations (27, 35–38) and that it can be ordered in different ways depending, for example, on whether or not the  $\gamma$  chain peptide is bound to the platelet fibrinogen receptor (38). This  $\gamma$  chain flexibility would also help to explain the formation of interfibrillar crosslinked  $\gamma$  trimers and  $\gamma$  tetramers, occurring in a setting of previously formed  $\gamma$  dimers (24) and is consistent with the fact that neither Yee *et al.* (27) nor Spraggon *et al.* (21) visualized this segment of the  $\gamma$  chain in their crystal structures. The idea that this region is flexible also is strongly suggested by our present observation that C-terminal  $\gamma$  chains are situated in several locations in the D domain ranging from distal to proximal.

The C-terminal region of the  $\gamma$  chain emerges 3.5 nm from the gly-pro-arg-pro-binding pocket at the distal end of the D domain (cf., Fig. 1) (27). Thus, gold clusters in proximal regions of the D domain of fibrinogen or fibrin and most proximal clusters in the middle region (i.e., >4 nm from the distal end) indicate the presence of terminal  $\gamma$  chains that are oriented toward the central E domain of fibrinogen (68% of the total), suitably situated between the strands of a fibrin fibril for transverse crosslinking to take place. The most proximally located clusters were 8.1–11.3 nm from the distal end of the D domain (34% of the total), indicating that  $\gamma$  chains in fibrinogen can extend further from their origin in the middle of the  $\gamma$  chain subdomain than was believed could plausibly occur based on measurements of D domain crystal structures (21, 27). Those gold clusters located 9.5 nm or more from the distal end of the molecule satisfy the distance requirement for two  $\gamma$  chains to be able to bridge transversely between  $\gamma_{406K}$  of one chain and  $\gamma_{398/399Q}$  of the other, notwithstanding an uncertainty of up to 1.5 nm regarding the location of the Au<sub>11</sub> cluster relative to the  $\gamma_{398/399}$  position (Fig. 2). This point cannot be addressed directly because of our experimental design, which precludes crosslinking of cadaverine-labeled  $\gamma$  chains. However, the more relevant feature of middle and proximally situated Au<sub>11</sub> clusters is that the  $\gamma$  chains to which they are attached are pointing away from the distal end of the molecule. This type of alignment is inconsistent with an end-to-end fibrin-crosslinking mechanism because distally oriented  $\gamma$  chains would be necessary for bridging to take place at adjacent ends of fibrin(ogen) molecules.

Yee *et al.* (27) suggested that transverse crosslinking is unlikely based on their calculation of the distance required for

$\gamma$  chains to reach halfway between the D domains from their emergence at  $\gamma_{392}$ , 3.5 nm from the gly-pro-arg-binding pocket at the extreme end of the molecule. Spraggon *et al.* (17) used similar reasoning based on observations of a crosslinked D dimer fragment. Although they were unable to visualize the crosslinked  $\gamma$  chains in their D dimer fragment, it was nevertheless obvious that the crosslinked C-terminal  $\gamma$  chains traversed the abutting D domains and thus were oriented end-to-end. They extrapolated these observations on the D dimer fragment to include the presumed position of crosslinked  $\gamma$  chains in assembled fibrin polymers and thus concluded that transverse crosslinking in fibrin polymers was not possible.

Crystallographic studies have without doubt provided important details on the folding and conformation of the fibrinogen D domain, but the relationships that are found in these isolated D fragments, especially as they concern the location of the C-terminal regions of  $\gamma$  chains, are not likely to be the ones that most often exist in fibrin and fibrinogen fibrils. Certain factors that play an important role in fibrinogen and fibrin assembly that affect the position of the C-terminal regions of  $\gamma$  chains include the intramolecular spacing that exists between D and E domains in fibrinogen and fibrin and the noncovalent D:E:D intermolecular interactions that occur uniquely among fibrin molecules.

We believe that existing biochemical and ultrastructural evidence strongly support transverse  $\gamma$  chain crosslinking as a major crosslinking mechanism in fibrin. Our present observation that C-terminal regions of  $\gamma$  chains were sometimes found at the far ends of fibrinogen molecules, plus previous observations on the location of  $\gamma$  chains in fibrinogen dimers implies that end-to-end crosslink positioning between D domains also can occur. For example, end-to-end positioning is a virtual certainty as far as the crosslinked  $\gamma$  chains in the adjacent D domains of D dimers are concerned (21), including dimeric D domains in crosslinked D-fibrin-D complexes after dissociation with acetic acid (26). End-to-end  $\gamma$  chain arrangements probably also occur in end-to-end aligned fibrinogen dimers, such as were observed by Fowler *et al.* (20) or more recently by us (1). Other experimental systems by using fragment E (28) or a fragment E analog (29) as a template for assembling single-stranded fibrinogen fibrils also seem to favor formation of end-to-end crosslinks because they produce end-to-end fibrinogen alignments. However, side-to-side strand associations (i.e., double-stranded fibrils) also occurred commonly in images published by Veklich *et al.* (28). The occurrence of such fibrils under these conditions strongly suggests that transverse crosslinks also had formed, thus rendering ambiguous the hoped for extrapolation that  $\gamma$  chain crosslinking in fibrin is exclusively end-to-end. In summary, we conclude from this present report as well as from previously cited experiments, that transverse  $\gamma$  chain crosslinking predominates in assembled fibrinogen and fibrin fibrils. This event does not, however, preclude occasional end-to-end crosslinking within such assembled polymer structures, but that still remains to be shown directly.

Early phases of this study were supported by National Institutes of Health Grant HL-47000. These investigations also were supported by National Institutes of Health Grant RR-01777 and U.S. Department of Energy, Office of Health and Environmental Research. We are most grateful to Karen Higgins for graphic arts services.

1. Mosesson, M. W., Siebenlist, K. R., Hainfeld, J. F. & Wall, J. S. (1995) *J. Struct. Biol.* **115**, 88–101.
2. Chen, R. & Doolittle, R. F. (1971) *Biochemistry* **10**, 4486–4491.
3. Doolittle, R. F., Chen, R. & Lau, F. (1971) *Biochem. Biophys. Res. Comm.* **44**, 94–100.
4. Purves, L. R., Purves, M. & Brandt, W. (1987) *Biochemistry* **26**, 4640–4646.
5. Kloczewiak, M., Timmons, S. & Hawiger, J. (1983) *Thromb. Res.* **29**, 249–255.

6. Hainfeld, J. F. (1987) *Science* **236**, 450–453.
7. Wall, J. S. & Hainfeld, J. F. (1986) *Annu. Rev. Biophys. Biophys. Chem.* **15**, 355–376.
8. Milligan, R. A., Whittaker, M. & Safer, D. (1990) *Nature (London)* **348**, 217–221.
9. Wagenknecht, T., Berkowitz, J., Grassucci, R., Timerman, A. P. & Fleischer, S. (1994) *Biophys. J.* **67**, 2286–2295.
10. Gregori, L., Hainfeld, J. F., Simon, M. N. & Goldgaber, D. (1997) *J. Biol. Chem.* **272**, 58–62.
11. Zlotnick, A., Cheng, N., Stahl, S. J., Conway, J. F., Steven, A. C. & Wingfield, P. T. (1997) *Proc. Natl. Acad. Sci. USA* **94**, 9556–9561.
12. Mosesson, M. W., Siebenlist, K. R., DiOrio, J. P., Hainfeld, J. F., Wall, J. S., Soria, J., Soria, C. & Samama, M. (1986) in *Fibrinogen and its Derivatives*, eds Müller-Berghaus, G., Scheefers-Borchel, U., Selmayr, E. & Henschen, A. (Elsevier Science, Amsterdam), pp. 3–15.
13. McKee, P. A., Mattock, P. & Hill, R. L. (1971) *Proc. Natl. Acad. Sci. USA* **66**, 738–744.
14. Kanaide, H. & Shainoff, J. R. (1975) *J. Lab. Clin. Med.* **85**, 574–597.
15. Samokhin, G. P. & Lorand, L. (1995) *J. Biol. Chem.* **270**, 21827–21832.
16. Sobel, J. H. & Gawinowicz, M. A. (1996) *J. Biol. Chem.* **271**, 19288–19297.
17. Matsuka, Y. V., Medved, L. V., Migliorini, M. M. & Ingham, K. C. (1996) *Biochemistry* **35**, 5810–5816.
18. Lorand, L., Chenowith, D. & Gray, A. (1972) *Ann. N. Y. Acad. Sci.* **202**, 155–171.
19. Mosesson, M. W., Amrani, D. L. & Ménaché, D. (1976) *J. Clin. Invest.* **57**, 782–790.
20. Fowler, W. E., Erickson, H. P., Hantgan, R. R., McDonagh, J. & Hermans, J. (1981) *Science* **211**, 287–289.
21. Spraggon, G., Everse, S. J. & Doolittle, R. F. (1997) *Nature (London)* **389**, 455–462.
22. Selmayr, E., Thiel, W. & Müller-Berghaus, G. (1985) *Thromb. Res.* **39**, 459–465.
23. Selmayr, E., Deffner, M., Bachmann, L. & Müller-Berghaus, G. (1988) *Biopolymers* **27**, 1733–1748.
24. Mosesson, M. W., Siebenlist, K. R., Amrani, D. L. & DiOrio, J. P. (1989) *Proc. Natl. Acad. Sci. USA* **86**, 1113–1117.
25. Mosesson, M. W., Siebenlist, K. R., DiOrio, J. P., Matsuda, M., Hainfeld, J. F. & Wall, J. S. (1995) *J. Clin. Invest.* **96**, 1053–1058.
26. Siebenlist, K. R., Meh, D. A., Wall, J. S., Hainfeld, J. F. & Mosesson, M. W. (1995) *Thromb. Haemostasis* **74**, 1113–1119.
27. Yee, V. C., Pratt, K. P., Coté, H. C. F., Le Trong, I., Chung, D. W., Davie, E. W., Stenkamp, R. E. & Teller, D. C. (1997) *Structure* **5**, 125–138.
28. Veklich, Y., Ang, E. K., Lorand, L. & Weisel, J. W. (1998) *Proc. Natl. Acad. Sci. USA* **95**, 1438–1442.
29. Lorand, L., Parameswaran, K. N. & Murthy, S. N. P. (1998) *Proc. Natl. Acad. Sci. USA* **95**, 537–541.
30. Mosesson, M. W. & Sherry, S. (1966) *Biochemistry* **5**, 2829–2835.
31. Mosesson, M. W., Galanakis, D. K. & Finlayson, J. S. (1974) *J. Biol. Chem.* **249**, 4656–4664.
32. Finlayson, J. S., Mosesson, M. W., Bronzert, T. J. & Pisano, J. J. (1972) *J. Biol. Chem.* **247**, 5220–5222.
33. Lorand, L. & Gotoh, T. (1970) *Methods Enzymol.* **19**, 770–782.
34. Loewy, A. G., Dunathan, K., Kriel, R. & Wolfinger, H. L., Jr. (1961) *J. Biol. Chem.* **236**, 2615–2633.
35. Mayo, K. H., Burke, C., Lindon, J. H. & Kloczewiak, M. (1990) *Biochemistry* **29**, 3277–3286.
36. Blumenstein, M., Matsueda, G. R., Timmons, S. & Hawiger, J. (1992) *Biochemistry* **31**, 10692–10698.
37. Donahue, J. P., Patel, H., Anderson, W. F. & Hawiger, J. (1994) *Proc. Natl. Acad. Sci. USA* **91**, 12178–12182.
38. Mayo, K. H., Fan, F., Beavers, M. P., Eckardt, A., Keane, P., Hoekstra, W. J. & Andrade-Gordon, P. (1996) *Biochemistry* **35**, 4434–4444.